



ELSEVIER

Available online at www.sciencedirect.com

SCIENCE @ DIRECT®

Journal of Sound and Vibration 274 (2004) 421–432

JOURNAL OF
SOUND AND
VIBRATION

www.elsevier.com/locate/jsvi

Letter to the Editor

Wind vibration mitigation of long-span bridges in hurricanes

C.S. Cai*, S.R. Chen

*Department of Civil and Environmental Engineering, Louisiana State University, 3502 CEBA,
Baton Rouge, LA 70803, USA*

Received 17 January 2003; accepted 4 September 2003

1. Introduction

Despite the massive population growth in the south and southeast along the hurricane coast of the United States, the transportation infrastructure has not increased its capacity accordingly. Long-span bridges are usually the backbones of transportation lines along the coastal areas. When a hurricane is approaching, these long-span bridges sometimes have to be closed in order to ensure the safety of the bridge as well as the transportation on them due to excessive wind-induced vibrations, which however greatly reduces the capability of hurricane evacuation through the bridges.

To date, bridge vibration controls in high wind speeds have not been adequately addressed. Most previous control work dealt with the bridge buffeting under moderate wind speeds [1], along with some cases of flutter controls in high wind speeds [2]. While active control devices may provide satisfactory multi-objective control performance in a full range of wind speeds [3], their dependence on external energy supply has hindered their applications to the disaster evacuations. Recently, some aerodynamic controls using flaps were proposed to control flutter instability [4]. However, their applicability to buffeting control has not been reported and established.

Vehicles on bridges act as a sort of Spring–Damper-Subsystems (SDSs) to the bridge [5–7]. The SDS is used here as a general terminology to differentiate with Tuned Mass Dampers (TMDs). The former may or may not be pre-tuned, while the latter is pre-tuned to the “optimal” value (usually the fundamental frequency of the structural system) for efficient vibration control. The objective of the present study is to investigate the effects of different SDSs (with different vibration frequencies) on the bridge performance during hurricane evacuations and develop a truck-type of movable passive SDS. The passive nature makes the control approach more reliable than the active one, considering the reality that power may not be available during the hurricane disasters. The temporary/movable SDS can be conveniently driven on the existing bridges when necessary, and be removed when it is not needed.

*Corresponding author. Tel.: +1-225-578-8442; fax: +1-225-578-8652.

E-mail address: cscai@lsu.edu (C.S. Cai).

It has been reported that the gust wind speed during hurricanes could be up to 60–80 m/s or more in the United States and other areas [9,10]. Though the duration may be short, the consequence of such strong winds may be catastrophic for both the safety of the bridge and the safety of traffic on the bridge.

The flutter instability problem is the most critical wind-related issue for long-span bridges. It has been known that hurricane-induced strong winds have much higher turbulence intensity than that of moderate winds. The effects of turbulence on the flutter stability are still controversial [11,12] and a non-linear aerodynamic analysis by Chen et al. [13] confirmed that turbulence might destabilize the bridge. Before fully understanding the turbulence effect, raising the flutter instability limit of the bridge to a conservative level, as proposed in the present study, seems to be an appropriate way to maintain the safety of the bridge.

For service performance, the main threat to the bridge and vehicles is the excessive acceleration response in the vertical and lateral directions when the bridge is subjected to strong winds. Lateral large acceleration may cause the overturning or loss of control of the vehicles [14,15]. The excessive acceleration in vertical direction may cause the discomfort problems of drivers and passengers [16]. Therefore, effectively reducing the acceleration response of the bridge may maximize the transportation capacity and possibly save lives and properties in hurricane-prone areas.

Irwin [16] suggested the following control guidelines:

- When wind speed $U \leq 13$ m/s, peak vertical acceleration should be no more than $0.05g$ (g = gravity acceleration).
- When wind speed $U > 13$ m/s, peak vertical acceleration should be no more than $0.1g$.

2. Equations of motion of bridge–SDS system

There are a variety of vehicle configurations during evacuations. Typically, a vehicle model is composed of several rigid bodies connected by a series of springs, damping devices, and pivots [5]. This kind of model can have over 10 degree-of-freedom [6]. For simplicity, usually models with fewer degree-of-freedom have been adopted [5] and a single-degree-of-freedom (SDOF) model has been proven acceptable when the overall dynamic performance of the bridge other than local dynamic problems of vehicles is of concern [7]. Therefore, in evaluating the vehicle effects on the dynamic performance of bridges under wind actions, a SDOF Spring–Damping Subsystem (SDOF-SDS) model is selected to represent the vehicle, as shown in Fig. 1. This SDS model consists of a rigid body representing the mass of the whole vehicle; a spring representing the stiffness supplied by the suspension system and the tires; and a damping pot representing the damping effect from the damping system of the vehicle and the tires.

For the model shown in Fig. 2, assuming that a bridge has a displacement of $r(x, t)$ consisting of $h(x)$ in vertical direction, $p(x)$ in lateral direction, and $\alpha(x)$ in torsion direction, and wind forces consisting of buffeting force $f_b(x, t)$ and the aeroelastic self-excited force $f_s(x, r, \dot{r})$. Assuming also that a total number of n_1 modes are included in the analysis and a total number of n_2 SDSs are attached to the bridge at location x_s ($s = 1$ to n_2). For each mode, vibrations in three directions h , p and α are considered. For the case without SDS, the following derivation reduces back to the

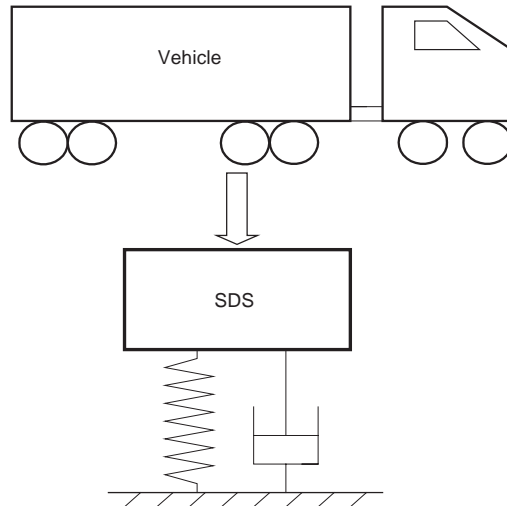


Fig. 1. Simplified SDS model for vehicles.

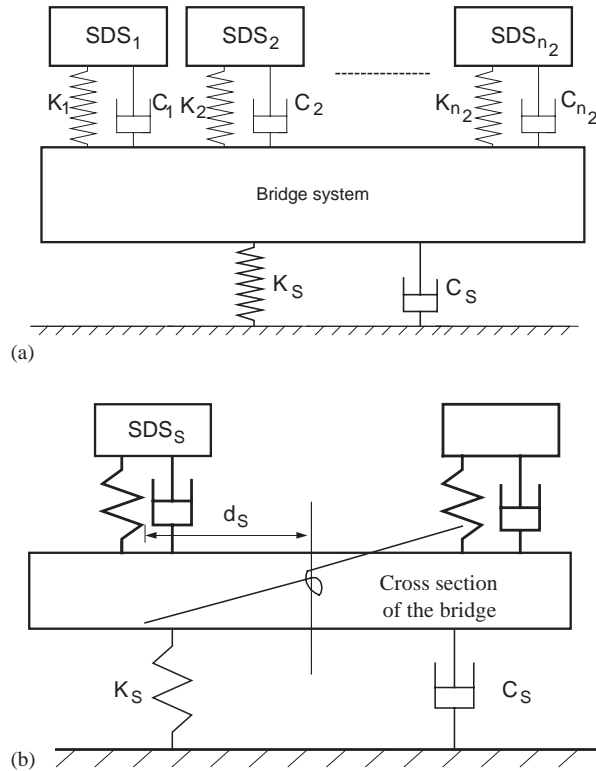


Fig. 2. Bridge system attached with multiple SDS. (a) Outline of bridge-SDS system (elevation) and (b) cross-section of the bridge.

formulation of Ref. [8]. Therefore, the reader is referred to Ref. [8] for the detailed aerodynamic loading models and mathematical derivations. The equations of motion for the bridge–SDS system can be derived as

$$\mathbf{M}\boldsymbol{\eta}'' + \mathbf{C}\boldsymbol{\eta}' + \mathbf{S}\boldsymbol{\eta} = \mathbf{F}, \tag{1}$$

where

$$\boldsymbol{\eta} = \{\xi_1, \dots, \xi_{n_1}, \gamma_1, \dots, \gamma_{n_2}\}^T, \tag{2}$$

$$\mathbf{M} = \begin{bmatrix} M_{n_1 \times n_1}^1 & M_{n_1 \times n_2}^2 \\ M_{n_2 \times n_1}^3 & I_{n_2 \times n_2}^{unit} \end{bmatrix}, \tag{3}$$

$$\mathbf{C} = \begin{bmatrix} C_{n_1 \times n_1}^1 & 0 \\ 0 & C_{n_2 \times n_2}^2 \end{bmatrix}, \quad \mathbf{S} = \begin{bmatrix} S_{n_1 \times n_1}^1 & 0 \\ 0 & S_{n_2 \times n_2}^2 \end{bmatrix}, \quad \mathbf{F} = \{Q_b, 0 \dots 0\}, \tag{4-6}$$

and where $\boldsymbol{\eta}$ = vector of the generalized co-ordinate of the bridge–SDS system; ξ = generalized co-ordinate of the bridge; γ = co-ordinate of the vertical motion of SDSs; a superscript “T” represents transpose of vectors and a superscript prime “'” represents a derivative with respect to dimensionless time $s = Ut/B$; U is the wind velocity; t the physical time; B the bridge width; M , C , and S are the mass, damping, and stiffness matrices, respectively. The M consists of mass contributions from the bridge and SDS. The C and S consist of contributions from structural, aerodynamic, and SDS damping and stiffness; n_1 is the number of modes; n_2 the number of SDSs; I^{unit} the unit matrix; F the external force vector from wind buffeting, and Q_b the generalized buffeting force [8]. The components of the matrices are:

$$C_{ij}^1(K) = \frac{B}{U} \frac{2\zeta_i \omega_i \delta_{ij} - \rho_a B^4 \omega Z_{ij}}{(1 + \sum_{s=1}^{n_2} \mu_s^i)} \quad (i, j = 1 \dots n_1), \tag{7}$$

$$C_{n_2 \times n_2}^2 = \frac{B}{U} \text{diag} (2\zeta_1^1 \omega_1^1, 2\zeta_1^2 \omega_1^2, \dots, 2\zeta_{n_2}^2 \omega_{n_2}^2), \tag{8}$$

$$S_{ij}^1(K) = \frac{B^2}{U^2} \frac{\omega_i^2 \delta_{ij} - \rho_a B^4 \omega^2 T_{ij}}{(1 + \sum_{s=1}^{n_2} \mu_s^i)} \quad (i, j = 1 \dots n_1), \tag{9}$$

$$S_{n_2 \times n_2}^2 = \frac{B^2}{U^2} \text{diag} ((\omega_1^1)^2, (\omega_1^2)^2, \dots, (\omega_{n_2}^2)^2), \tag{10}$$

$$M_{ij}^1 = \frac{I_{ij} + \sum_{s=1}^{n_2} \int_0^l I_t^s r_i(x) r_j(x) dx}{I_{ii} (1 + \sum_{s=1}^{n_2} \mu_s^i)} \quad (i, j = 1 \dots n_1), \tag{11}$$

$$M_{ij}^2 = \frac{\int_0^l I_t^j r_i(x) dx}{I_{ii} (1 + \sum_{s=1}^{n_2} \mu_s^i)} \quad (i = 1 \dots n_1; j = 1 \dots n_2), \quad M_{ij}^3 = r_j(x_i) \tag{12, 13}$$

$$(i = 1 \dots n_2; j = 1 \dots n_1),$$

$$\mathbf{Z}_{ij} = H_1^* G_{h_i h_j} + H_2^* G_{h_i \alpha_j} + H_5^* G_{h_i p_j} + P_1^* G_{p_i p_j} + P_2^* G_{p_i \alpha_j} + P_5^* G_{p_i h_j} + A_1^* G_{\alpha_i h_j} + A_2^* G_{\alpha_i \alpha_j} + A_5^* G_{\alpha_i p_j}, \tag{14}$$

$$T_{ij} = H_4^* G_{h_i h_j} + H_3^* G_{h_i \alpha_j} + H_6^* G_{h_i p_j} + P_4^* G_{p_i p_j} + P_3^* G_{p_i \alpha_j} + P_6^* G_{p_i h_j} + A_3^* G_{\alpha_i \alpha_j} + A_4^* G_{\alpha_i h_j} + A_6^* G_{\alpha_i p_j}, \quad (15)$$

where δ_{ij} is the Kronecker delta function that is equal to 1 if $i = j$ and equal to 0 if $i \neq j$; ω_i and ζ_i the circular natural frequency and mechanical damping ratio of i th mode, respectively; ρ_a the air density; l the bridge length; H_i^*, P_i^*, A_i^* ($i = 1 - 6$) = experimentally determined flutter derivatives for the deck cross-section under investigation; and ζ_t^s and ω_t^s = damping ratio and circular natural frequency of the s th SDS, respectively. The modal integral ($G_{r_i s_j}$), the general mass moment inertia of the bridge (I_{ij}), and the generalized mass moment inertia ratio between the s th SDS and the i th mode (μ_s^i) are defined as

$$G_{r_i s_j} = \int_0^l r_i(x) s_j(x) dx, \quad I_{ij} = \int_0^l m(x) r_i(x) r_j(x) dx, \quad (16, 17)$$

$$\mu_s^i = \frac{\int_0^l I_t^s r_i^2(x) dx}{I_{ii}}, \quad (18)$$

where $r_i = h_i, p_i$ or α_i ; $s_j = h_j, p_j$ or α_j ; $I_t^s = m_s$ for the vertical and lateral modes or $I_t^s = m_s \times d_s^2$ for torsion mode; and d_s the horizontal distance between the s th SDS and the torsion center of the cross-section (see Fig. 2(b)); and $m(x)$ the mass per unit length for vertical and lateral modes; or $m(x)$ the mass moment of inertia per unit length for the torsion mode.

3. Solution of flutter and buffeting response

A carefully designed SDS system can increase the flutter critical wind speed for the combined bridge–SDS system. The homogenous part of Eq. (1) is expressed in the state-space format as

$$\mathbf{A}\dot{\mathbf{Y}} + \mathbf{B}\mathbf{Y} = \{\mathbf{0}\} \quad (19)$$

and the complex conjugate pairs of eigenvalues are obtained as

$$\lambda_{j,j+1} = -\zeta_j \omega_j \pm i \sqrt{1 - \zeta_j^2} \omega_j, \quad j = 1 \text{ to } (n_1 + n_2), \quad (20)$$

where λ_j , ω_j and ζ_j are eigenvalue, modal frequency and damping ratio of the j th mode, respectively; and i is the unit imaginary number ($i = \sqrt{-1}$). If the modal damping ratio ζ_j changes from positive to negative, the corresponding wind speed is identified as the flutter critical wind speed U_{cr} .

To evaluate the control performance, the control efficiency of flutter is defined with R_1 as

$$R_1 = \left(\frac{\hat{U}_{cr}}{U_{cr}} - 1 \right) 100\%, \quad (21)$$

where \hat{U}_{cr} and U_{cr} are flutter critical wind speed with and without SDS control, respectively.

To solve the buffeting response, Eq. (1) can then be Fourier transformed into a new system as

$$\mathbf{H}\bar{\eta} = \bar{\mathbf{F}}, \quad (22)$$

where $\bar{\eta}$ and \bar{F} = Fourier transformation of η and F , respectively; the impedance matrix \mathbf{H} has the general form of $H_{ij} = -\omega^2 M_{ij} + i\omega C_{ij}(\omega) + S_{ij}(\omega)$, where subscripts $i, j = 1$ to $(n_1 + n_2)$ and $i = \sqrt{-1}$.

The mean square of displacements in vertical, lateral and torsion directions is related to the buffeting force spectra $S_{Q_{b_i}Q_{b_j}}$ as follows:

$$\hat{\sigma}_r^2(x) = \sum_i \sum_j \delta_B^2 r_i(x)r_j(x) \int_0^\infty [H^{-1}]_{ij} S_{Q_{b_i}Q_{b_j}} [H^{-1}]_{ij}^T d\omega. \tag{23}$$

The control efficiency of buffeting displacement is defined with R_2 as

$$R_2 = \left(1 - \frac{\hat{\sigma}_r}{\sigma_r} \right) 100\%, \tag{24}$$

where $\hat{\sigma}_r$ and σ_r are the root-mean-square (RMS) of displacement with and without SDS control, respectively.

It is noted that in this exploratory analysis focusing on bridge performance, the direct dynamic wind effect on the vehicle is not considered. The main reasons are: first, its effect on bridge is relatively insignificant; second, wind load coefficients of the proposed truck type of SDS are not available. The wind on vehicle will be included in the on going research that focuses on vehicle performance. It is also noted that vehicles are attached to fixed points of the bridge without considering the dynamic movement of vehicle (consider only the vertical vibration with the bridge). This is to simulate two cases. First, the vehicle moves slowly during hurricane evacuation and the dynamic effect is insignificant. Second, the designed movable truck-type SDS is proposed to be placed (fixed) on the bridge. Dynamic interaction between moving vehicles and bridge is under study and the results will be reported in the future. Geometric non-linear effect of cables was considered in the static finite element analysis, which predicts the static deformation of the bridge.

4. Numerical example: Humen bridge–SDS system

To better demonstrate the applicability of the developed procedure, the Humen suspension bridge is analyzed. This bridge with a main span of 888 m is located in the south of China, where hurricane (typhoons) are a serious threat. The basic data of the bridge are shown in Table 1. Four

Table 1
Basic data of Humen suspension bridge

Main span (m)	888	Life force coefficient C_L at 0° attack angle	0.02
Bridge width (m)	35.6	Drag force coefficient C_D at 0° attack angle	0.84
Height of deck above water (m)	60	Torque coefficient C_M at 0° attack angle	0.019
Mass per unit length (10^3 kg/m)	18.34	$\partial C_L / \partial \alpha$ (0° attack angle)	0.51
Moment inertia per unit length (10^3 kg/m)	1743	$\partial C_M / \partial \alpha$ (0° attack angle)	0.62
Design wind speed (m/s)	57.2	Structural damping ratio	0.005
First symmetric vertical mode (Hz)	0.17	First symmetric torsion mode (Hz)	0.36
First asymmetric vertical mode (Hz)	0.28	First asymmetric torsion (Hz)	0.43

modes (two symmetric and two asymmetric) are listed in Table 1 [17]. Existent analysis has shown that the mid-point of the main span has the largest vibration response and the first symmetric vertical bending mode and the first symmetric torsion mode are the two modes most prone to couple together. Therefore, these two symmetric modes are the most important modes for buffeting response (asymmetric modes contribute nearly nothing at the mid-span point) and flutter instability. For simplicity and for demonstration purpose, only these two symmetric modes are considered in the evaluation of the SDS control efficiency for bridge flutter instability and buffeting response. The mass of the SDS, expressed as the percentage of the bridge mass, ranges from 1.0% to 1.5% in the present study.

Using the complex eigenvalue modal analysis approach introduced earlier, the flutter instability of the bridge—SDS system was analyzed with varied frequencies of the SDS. It is found in Fig. 3 that when the frequency of the SDS is very low (close to zero), the SDS is actually acting as a static mass block on the bridge. Since the SDS is placed on one side of the cross-section at the mid-point of the span, it acts essentially as a static eccentric load when its frequency approaches to zero. In the case of 1% mass ratio, the flutter critical wind velocity can be improved from about 87 m/s (without SDS) to 93 m/s ($R_1 = 7\%$). Such a result also agrees with the conclusion that an eccentric mass can increase the flutter stability of the bridge [2]. However, when the SDS frequency becomes quite high (larger than 0.5 Hz), the SDS has no effect on the flutter stability at all as reflected by the flat horizontal line that corresponds to the case without SDS ($U_{cr} = 87$ m/s). The same tendency can also be observed in the cases of larger mass ratios (1.25% and 1.5%). These results suggest that the vibration of traditional vehicles may have an insignificant effect on the flutter instability of bridges under wind action since the frequency of the vehicles (normally over 1.0 Hz) is relatively too high to affect the bridge stability. Fig. 3 also indicates that the optimal SDS frequency is about 0.25 Hz. This frequency corresponds to the torsion modal oscillation frequency (modified from the natural frequency by aerodynamic forces).

Fig. 4 shows the acceleration peak response under different wind speeds in cases with and without SDS control for the case of 1.25% mass ratio with optimal SDS frequency (0.25 Hz, determined from flutter analysis). As expected, the service criteria (indicated by the horizontal

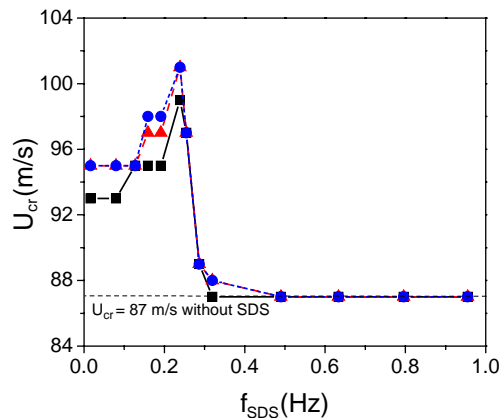


Fig. 3. Flutter critical wind velocity versus SDS frequency (generalized mass ratio = \blacksquare —, 1%; \blacktriangle —, 1.25%; \bullet —, 1.5%).

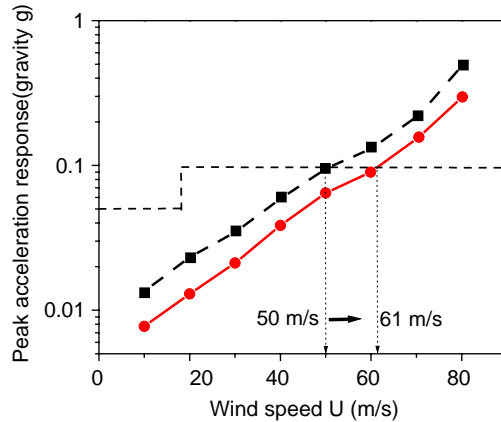


Fig. 4. Peak acceleration response versus wind velocity (—■—, uncontrolled; —●—, controlled).

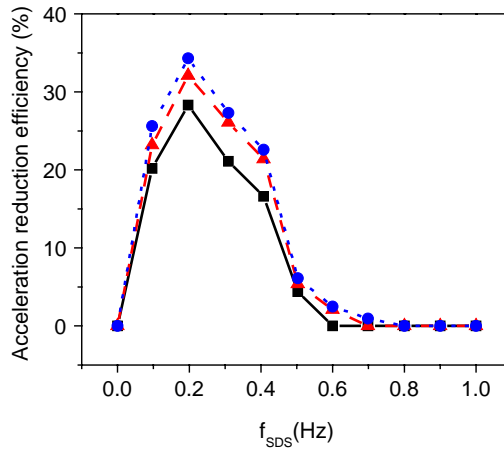


Fig. 5. Acceleration reduction ratio versus SDS frequency at $U = 60$ m/s (generalized mass ratio = —■—, 1%; —▲—, 1.25%; —●—, 1.5%).

dash lines) can be satisfied in a higher wind speed when SDS is used. More specifically, for the same control criteria, the service wind speed limit is raised from originally 50 m/s (without SDSs) to 61 m/s (with SDSs).

Fig. 5 shows the acceleration reduction ratio versus the different SDS frequencies under a wind speed of 60 m/s. It is found that the maximum reduction ratio can be about 28%, 32%, and 35% for the SDS mass ratio of 1.0%, 1.25%, and 1.5%, respectively. However, the SDS with high or low frequency has a small reduction effect on the buffeting (acceleration) response. This means that, similarly to the flutter instability, typical vehicles may have no significant effect on the buffeting response of the bridge since the vibration frequency of a typical vehicle is larger than 1.0 Hz. Only a well-designed SDS with its frequency tuned to the optimal one will have an efficient control effect on the vertical accelerations. In this particular example, the SDS should have a

frequency around 0.2 Hz for an optimal buffeting control for wind velocity of 60 m/s. In that case, the SDS with a pre-tuned frequency becomes a kind of TMD.

The numerical results discussed above have shown that a well-designed SDS system can raise flutter velocity and reduce buffeting vibrations. Movable SDS control devices are thus specifically designed for extreme situations when a hurricane forecast is made and the control need is identified. The preliminary design concept of a vehicle-type of control approach is introduced as follows.

To avoid the problem of vehicle instability or lateral overturning, the proposed vehicle-type of SDS (Fig. 6) has almost the same height as a typical truck. Lever-type design [3], which can greatly reduce the required vertical clearance of a typical vertical control device, is adopted here. The mass block uses iron to minimize the required space. Each vehicle-type of SDS has a gross mass of 10,000 kg. The dimensions of a vehicle-type of SDS can be seen in Fig. 6(a). The SDSs can be spread along the bridge as shown in Fig. 6(b), which is similar to the case of traditional multiple tuned mass dampers (MTMDs).

As in the case of designing MTMDs, the optimal frequency bandwidth ratio (B_f), the ratio of the central frequency of MTMD series (f_{av}) to the modal frequency of the concerned mode, and the damping ratio are the three main design variables [1]. Optimal variables can usually be obtained through numerical searching. There are also some approximate design formulas to help attain the optimal frequency bandwidth ratio and central frequency of MTMDs [18]. The

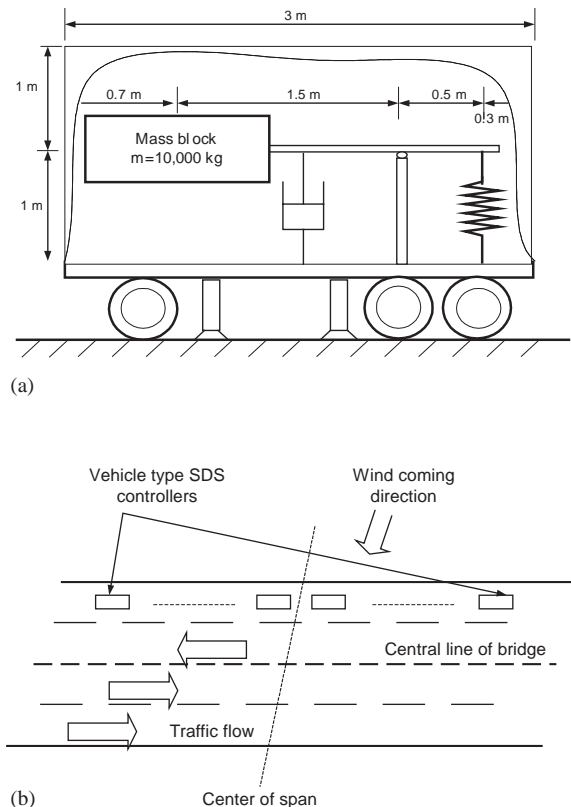


Fig. 6. Outline of movable SDSs: (a) Vehicle-type SDS controller and (b) placement of SDS on bridges.

Table 2
Optimal variables of SDS for Humen suspension bridge

Number of SDS (n_2)	Gen. mass ratio (%)	f_{av}/f_z	B_f	ζ_t	New U_{sev}^a (m/s)	New U_{cr}^b (m/s)
(a) <i>One lane placement</i>						
10	0.8	0.94	0.15	0.06	55	92
16	1.25	0.93	0.16	0.05	61	99
20	1.6	0.93	0.16	0.05	68	110
26	2.1	0.93	0.18	0.04	74	115
(b) <i>Two lanes placement</i>						
10	0.8	0.95	0.15	0.06	60	95
16	1.25	0.95	0.15	0.06	67	103
20	1.6	0.95	0.16	0.05	73	112
26	2.1	0.94	0.16	0.05	78	117

^a U_{sev} without SDS equals to 50 m/s.

^b U_{cr} without SDS equals to 87 m/s.

procedure of searching optimal variables is not repeated here and the reader can be referred to Refs. [1,18].

The number of SDSs is directly related to the control effect and the investment on control facilities. Using the Humen bridge as example, Table 2 compares the control efficiencies corresponding to one-lane and two-lane SDS placements and various numbers of SDSs. All of the optimal design variables with respect to different numbers of SDSs are listed in the table as well. In the table, $B_f = (f_{highest} - f_{lowest})/f_{av}$ is the bandwidth ratio of the even frequency distribution of SDSs ($f_{highest}$ and f_{lowest} are the highest and lowest frequencies among all SDSs, respectively), f_{av} is the average frequency of multiple SDSs and ζ_t is the damping ratio for all of the SDSs. The control performances are quantified using two variables: the new U_{sev} and the new U_{cr} . The former is the new service wind velocity limit under which service criteria shown in Fig. 4 can be satisfied and the latter is the new critical flutter wind velocity with SDSs. It has been shown in Table 2 that the control performance basically changes positively with the increase of the numbers of SDSs and for most cases, significant control effects can be observed.

It is noted that this exploratory research is to investigate an alternative to improve the bridge performance in extreme events for long-span bridges during hurricanes. Placement of movable SDS system on bridge during evacuation will certainly block traffic and is not a perfect solution. However, it is better than otherwise to completely close a bridge in evacuation or see the bridge being damaged or collapse. In an extreme case, to protect the bridge otherwise from being damaged or failure, the movable SDSs can also be placed on the bridge when the bridge is completely closed to traffic. Certainly, some issues as how to fix the movable SDSs on the bridge under strong wind need to be addressed before actual implementation.

5. Conclusion

To maximize the service capability and maintain the safety of the bridge itself, a movable/temporary passive control approach has been proposed based on a general formulation of the

bridge–SDS system. The effect of vehicles on the dynamic performance of long-span bridges subjected to wind action is then investigated with the Humen suspension bridge. The following conclusions can be drawn:

(1) A well-designed movable vehicle-type of control facility can effectively and conveniently increase the maximum wind velocity limit for bridge service in hurricane evacuations. For the case of 1.0% mass ratio, it reduces the peak acceleration by around 28% and simultaneously increases the flutter critical wind speed by about 14%.

(2) Typical vehicles have no significant effects on the bridge flutter stability and peak response of acceleration. This is due to the fact that vehicle's vibration frequency is relatively too high compared with that of the bridge's fundamental/important modes. However, it should be noted that the wind effect on the traffic is not considered in the present study. The existence of traffic on the bridge may significantly modify the aerodynamic characteristics of the bridge section. Including these factors may change the bridge performance. Work on these issues is being undertaken by the writers and will be presented in the future.

(3) It is noted that this exploratory research is to investigate an alternative to improve the bridge performance in extreme events for long-span bridges during hurricanes. Placement of a movable SDS system on a bridge during evacuation will certainly block traffic and is not a perfect solution. However, it is better than to completely close the bridge to evacuation. In an extreme case, to protect the bridge from being damaged or failure, the movable SDSs can also be placed on the bridge when the bridge is completely closed to traffic. Some issues for practical implementation certainly need to be further addressed.

Acknowledgements

This work is partially supported by the Louisiana State University and NSF Grant CMS-0301696.

References

- [1] M. Gu, S.R. Chen, C.C. Chang, Parametric study on multiple tuned mass dampers for buffeting control of Yangpu Bridge, *Journal of Wind Engineering and Industrial Aerodynamics* 89 (11–12) (2001) 987–1000.
- [2] S. Phongkumsing, K. Wilde, Y. Fujino, Analytical study on flutter suppression by eccentric mass method on FEM model of long-span suspension bridge, *Journal of Wind Engineering and Industrial Aerodynamics* 89 (2001) 515–534.
- [3] M. Gu, S.R. Chen, C.C. Chang, Control of wind-induced vibrations of long-span bridges by semi-active lever-type TMD, *Journal of Wind Engineering and Industrial Aerodynamics* 90 (2) (2002) 111–126.
- [4] K. Wilde, Y. Fujino, T. Kawakami, Analytical and experimental study on passive aerodynamic control of flutter of a bridge deck, *Journal of Wind Engineering and Industrial Aerodynamics* 80 (1999) 105–119.
- [5] W.H. Guo, Y.L. Xu, Fully computerized approach to study cable-stayed bridge–vehicle interaction, *Journal of Sound and Vibration* 248 (4) (2001) 745–761.
- [6] K. Park, S. Heo, I. Baek, Controller design for improving lateral vehicle dynamic stability, *JSAE Review* 22 (2001) 481–486.
- [7] M. Zaman, M.R. Taheri, A. Khanna, Dynamic response of cable-stayed bridges to moving vehicles using the structural impedance method, *Applied Mathematical Modeling* 20 (1996) 877–889.

- [8] A. Jain, N.P. Jones, R.H. Scanlan, Coupled flutter and buffeting analysis of long-span bridges, *Journal of Structural Engineering, American Society of Chemical Engineers* 122 (7) (1996) 716–725.
- [9] J.L. Schroeder, D.A. Smith, R.E. Peterson, Variation of turbulence intensities and integral scales during the passage of a hurricane, *Journal of Wind Engineering and Industrial Aerodynamics* 77&78 (1998) 65–72.
- [10] R.N. Sharma, P.J. Richards, A re-examination of the characteristics of tropical cyclone winds, *Journal of Wind Engineering and Industrial Aerodynamics* 83 (1999) 21–33.
- [11] C.S. Cai, P. Albrecht, H.R. Bosch, Flutter and buffeting analysis. I: Finite-element and RPE solution, *Journal of Bridge Engineering, American Society of Chemical Engineers* 4 (3) (1999) 174–180.
- [12] C.S. Cai, P. Albrecht, H.R. Bosch, Flutter and buffeting analysis. II: Luling and deer isle bridges, *Journal of Bridge Engineering, American Society of Chemical Engineers* 4 (3) (1999) 181–188.
- [13] X. Chen, A. Kareem, F.L. Haan, Nonlinear aerodynamic analysis of bridges under turbulent winds: the new frontier in bridge aerodynamics, *Proceedings of the International Conference on Advances in Structural Dynamics (ASD 2000)*, Hong Kong, China, December 2000, pp. 475–482.
- [14] J. Baker, The quantification of accident risk for road vehicles in cross winds, *Journal of Wind Engineering and Industrial Aerodynamics* 52 (1994) 93–107.
- [15] R. Sigbjornsson, J.T. Snabjornsson, Probabilistic assessment of wind related accidents of road vehicles: a reliable approach, *Journal of Wind Engineering and Industrial Aerodynamics* 74–76 (1998) 1079–1090.
- [16] P.A. Irwin, Motion criteria, Technical notes of the Rowan Williams Davies & Irwin Inc. (RWDI), Ontario, Canada, 1991.
- [17] L.Z. Xin, H.F. Xiang, Full-scale wind tunnel experiment of Humen Bridge, Technical report of State Key Laboratory of Wind Tunnel in China, 1995 (in Chinese).
- [18] A. Kareem, S. Kline, Performance of multiple mass dampers under random loading, *Journal of Structural Engineering, American Society of Chemical Engineers* 121 (SE2) (1994) 349–361.